

Electromagnetic interactions in elastic neutrino-nucleon scattering

Konstantin A. Kouzakov

*Department of Nuclear Physics and Quantum Theory of Collisions,
Faculty of Physics, Lomonosov Moscow State University, Moscow 119991, Russia**

Fedor M. Lazarev and Alexander I. Studenikin

*Department of Theoretical Physics, Faculty of Physics,
Lomonosov Moscow State University, Moscow 119991, Russia[†]*

(Dated: December 4, 2024)

arXiv:2412.02169v1 [hep-ph] 3 Dec 2024

Abstract

A thorough account of electromagnetic interactions of massive Dirac neutrinos as well as their spin-flavor state in the theoretical formulation of elastic neutrino-nucleon scattering is given. The formalism of neutrino charge, magnetic, electric, and anapole form factors defined as matrices in the mass basis is employed under the assumption of three-neutrino mixing. The flavor and spin change of neutrinos propagating from the source to the detector is taken into account in the form of a spin-flavor density matrix of the neutrino arriving at the detector. The potential effects of the neutrino charge radii, magnetic moments, and spin polarization in the neutrino-nucleon scattering experiments are outlined.

I. INTRODUCTION

Nonzero masses and mixing of neutrinos indicate that they have properties and interactions beyond the Standard Model (SM), in which neutrinos can couple to W^\pm and Z^0 bosons only. In view of this, searches for neutrino electromagnetic (EM) properties are of particular interest [1–3]. Indeed, it is known that the neutrino charge radii are predicted to be nonzero even within the SM [4–6], while nonzero neutrino magnetic moments arise already in the minimally extended SM [7]. Also, the beyond-SM theories discuss properties of right-handed neutrinos [8]. In the present study, we consider the most general case of Dirac neutrino EM properties: in addition to the charge radius and magnetic moment, we take into account the electric millicharge and anapole and electric dipole moments.

The effects of neutrino EM properties can manifest themselves both in astrophysical processes, where neutrinos propagate in strong magnetic fields and dense matter, and in laboratory experiments that employ neutrino fluxes from various sources. In the latter case, measurements of cross sections for neutrino scattering on various targets are a rather sensitive and widely used method. For example, Alvarez Ruso *et al* [9] and Chen [10] discussed neutrino-nucleon scattering at various energies and emphasized that precise theoretical calculations are required to meet the needs of experiments. In order to study experimentally processes of neutrino-nucleon and neutrino-nucleus scattering, it is also necessary to take

* kouzakov@srd.sinp.msu.ru

† lazarev.fm15@physics.msu.ru

into account radiative corrections [11–14] and details of the inner structure of nucleons and nuclei for both elastic [15–17] and inelastic [18] collisions.

In recent years, great attention has been drawn to coherent elastic neutrino–nucleus scattering ($\text{CE}\nu\text{NS}$), which was predicted half a century ago [19, 20] and which was first experimentally registered in 2017 by the COHERENT collaboration [21]. $\text{CE}\nu\text{NS}$ is not only a new tool for studying neutrino properties, but it also permits probing the structure of nuclei [22–24]. Moreover, the $\text{CE}\nu\text{NS}$ process may contribute to the background signal in the experiments searching for dark-matter particles.

Effects of neutrino EM interactions are among expected manifestations of new physics in the $\text{CE}\nu\text{NS}$ experiments. The data from the $\text{CE}\nu\text{NS}$ experiments, such as COHERENT, CONUS, and Dresden-II, were already used to set limits on the neutrino millicharge, charge radius, and magnetic moment [14, 25–29]. Data from a number of other new experiments aimed at studying $\text{CE}\nu\text{NS}$ are expected to appear in the near future. In order to study neutrino EM properties in $\text{CE}\nu\text{NS}$ experiments, it is necessary to develop a theoretical formalism that would take into account various neutrino and nuclear EM form factors. It is reasonable to begin solving this problem by considering elastic neutrino scattering on the basic constituent of a nucleus, namely a nucleon. Besides, a positively charged nucleon, i.e., a proton, is the simplest nuclear target. It should be also noted in this connection that elastic neutrino-proton scattering is a promising tool for detecting neutrinos from supernovas [30].

The most studied among the neutrino EM properties is the neutrino magnetic moment. One of its marked manifestations is neutrino spin oscillations in a magnetic field. This effect can be significant both in the environments of neutron stars and supernovas and in interstellar and/or intergalactic magnetic fields (see, for instance, Refs. [31, 32] and references therein). Such oscillations affect not only the flavour composition of neutrino fluxes but also the neutrino spin state. This means that a consistent treatment of the neutrino magnetic moment effects in the EM neutrino-nucleon scattering should also account for the neutrino spin polarization due to the neutrino spin oscillations on the source-detector distance.

The paper is organized as follows. In Sec. II, we discuss the structure of the vertex function for a spin-1/2 particle, taking into account weak neutral form factors for nucleons and EM form factors for nucleons and neutrinos and present a parametrization of the nucleon form factors, which are used further in numerical calculations. In Sec. III, we calculate the cross section for elastic neutrino–nucleon scattering under conditions characteristic of neutrino

scattering experiments. In Sec. IV, we discuss the results of numerical calculations for the neutrino-nucleon cross sections with different initial neutrino spin states on the basis of the formulas obtained for various values of neutrino EM properties and compare them with respective SM predictions. Section V summarizes this work.

II. NEUTRINO AND NUCLEON FORM FACTORS

Let us briefly touch upon a general approach to describing the properties of EM and weak interactions of spin-1/2 fermions (for a detailed treatment of this issue in the case of neutrino EM interactions, we refer the interested reader to Ref. [1]). The parameters of the fermion-photon and fermion- Z^0 boson interactions are specified by the vertex function $\Lambda_\mu^{fi}(p_i, p_f)$, where $p_{i(f)}$ is the momentum of the initial (final) spin-1/2 particle with mass $m_{i(f)}$. This vertex function determines the matrix element of the fermionic current

$$\langle p_f | j_\mu(0) | p_i \rangle = \bar{u}_f(p_f) \Lambda_\mu^{fi}(q, l) u_i(p_i), \quad (1)$$

where $u_i(p_i)$ and $u_f(p_f)$ are bispinor amplitudes for a free particle. Employing $q^\mu = p_i^\mu - p_f^\mu$, $l^\mu = p_i^\mu + p_f^\mu$, the metric tensor $g^{\mu\nu}$, and the Levi-Cevita antisymmetric tensor $\varepsilon^{\mu\nu\alpha\beta}$, the 4×4 matrix $\Lambda_\mu^{fi}(q, l)$ can be presented as a linear combination of the 16 matrices $\mathbb{1}$, γ_5 , γ^μ , $\gamma^\mu\gamma_5$ and $\sigma^{\mu\nu} = \frac{i}{2}[\gamma^\mu, \gamma^\nu]$. From hermiticity of the current operator $j_\mu^\dagger = j_\mu$ it follows that

$$[\Lambda_\mu^{fi}(q, l)]^\dagger = \gamma^0 \Lambda_\mu^{if}(-q, l) \gamma^0. \quad (2)$$

After using the Gordon-like identities one arrives at [33]

$$\begin{aligned} \Lambda_\mu^{fi}(q) = & f_1^{fi}(q^2) q_\mu + f_2^{fi}(q^2) q_\mu \gamma_5 + f_3^{fi}(q^2) \gamma_\mu + f_4^{fi}(q^2) \gamma_\mu \gamma_5 + f_5^{fi}(q^2) \sigma_{\mu\nu} q^\nu \\ & + f_6^{fi}(q^2) \varepsilon_{\mu\nu\alpha\beta} q^\nu \sigma^{\alpha\beta}. \end{aligned} \quad (3)$$

By virtue of the requirement of Lorentz invariance, the six form factors $f_{1,2,3,4,5,6}^{fi}(q^2)$ appearing here are functions of q^2 . Of them, $f_{2,3,4}^{fi}(q^2)$ are hermitian matrices, while $f_{1,5,6}^{fi}(q^2)$ are antihermitian.

In the case of the EM current, the gauge invariance implies the current conservation $\partial_\mu j^\mu = 0$, so that

$$q^\mu \bar{u}_f(p_f) \Lambda_\mu^{fi}(q, l) u_i(p_i) = 0. \quad (4)$$

This condition (along with the Gordon-like identities) leads to

$$f_1^{fi} q^2 + f_3^{fi} (m_f - m_i) = 0, \quad f_2^{fi} q^2 + f_4^{fi} (m_f + m_i) = 0. \quad (5)$$

Therefore, the EM vertex acquires the form

$$\Lambda_\mu^{(\text{EM})fi}(q) = \left(\gamma_\mu - \frac{q_\mu \not{q}}{q^2} \right) \left[f_3^{fi}(q^2) - \frac{q^2}{m_i + m_f} f_2^{fi}(q^2) \gamma_5 \right] + \sigma_{\mu\nu} q^\nu [f_5^{fi}(q^2) - 2i f_6^{fi}(q^2) \gamma_5]. \quad (6)$$

A. Neutrino EM form factors

From expression (6) it follows that the neutrino EM vertex function can be recast as (see also Ref. [1])

$$\Lambda_\mu^{(\text{EM};\nu)fi}(q) = (\gamma_\mu - q_\mu \not{q}/q^2) [f_Q^{fi}(q^2) + f_A^{fi}(q^2) q^2 \gamma_5] - i \sigma_{\mu\nu} q^\nu [f_M^{fi}(q^2) + i f_E^{fi}(q^2) \gamma_5], \quad (7)$$

where f_Q^{fi} , f_A^{fi} , f_M^{fi} and f_E^{fi} are, respectively, the charge, anapole, magnetic, and electric form factors of the diagonal ($f = i$) and transition ($f \neq i$) types in the basis of neutrino mass eigenstates. According to the hermiticity condition (2), we have

$$f_{Q,A,M,E}^{fi}(q^2) = (f_{Q,A,M,E}^{fi}(q^2))^*. \quad (8)$$

In the interaction with a real photon ($q^2 = 0$), the EM form factors determine stationary properties of neutrinos:

$$f_Q^{fi}(0) = e_{fi}, \quad 6 \left. \frac{df_Q^{fi}(q^2)}{dq^2} \right|_{q^2=0} = \langle r_{fi}^2 \rangle, \quad f_A^{fi}(0) = a_{fi}, \quad f_M^{fi}(0) = \frac{\mu_{fi}}{2m_e}, \quad f_E^{fi}(0) = \frac{\epsilon_{fi}}{2m_e}, \quad (9)$$

where e_{fi} , $\langle r_{fi}^2 \rangle$, a_{fi} , μ_{fi} and ϵ_{fi} are, respectively, the neutrino millicharge (in the units of elementary charge e_0), charge radius¹ and anapole moment (both are usually measured in cm^2), magnetic and electric dipole moments (in the units of Bohr magneton μ_B).

The neutrino EM form factors play a fundamental role. In particular, the neutrino EM properties may shed light on whether neutrinos are Dirac or Majorana particles: for example, Dirac neutrinos may have both diagonal and off-diagonal charge, magnetic, and electric form factors, while Majorana neutrinos may have only off-diagonal form factors of these types.

Among neutrino EM properties, the magnetic and electric dipole moments have been most studied theoretically. For the diagonal magnetic and electric dipole moments of the

¹ This term is commonly used in the literature for the mean-square charge radius.

Dirac neutrino, the minimally extended SM, which takes into account massive right-handed neutrinos, predicts the values [7]

$$\mu_{kk}^D \approx 3.2 \times 10^{-19} \mu_B \left(\frac{m_k}{1 \text{ eV}} \right), \quad \epsilon_{kk}^D = 0, \quad (10)$$

where μ_B is the Bohr magneton. Because of proportionality to the neutrino masses, the magnetic moments are many orders of magnitude smaller than the current experimental limits: $\mu_\nu \lesssim 10^{-12} - 10^{-11} \mu_B$ (see [34]). Nevertheless, these EM properties are a subject of searches in various experiments, since some theories beyond the minimally extended SM predict much greater values for them. Also, we would like to indicate the mechanism underlying the appearance of the induced magnetic moment of a massive neutrino that moves in a dense degenerate electron gas. The effective value of this magnetic moment may be several orders of magnitude greater than the value in Eq. (10) (see Refs. [35, 36] for details).

The neutrino charge and anapole form factors are also of interest. The possible existence of a nonzero neutrino electric charge (millicharge) is considered in some theories beyond the SM. Even if the millicharge is zero, the neutrino may have a nonzero charge radius, which contributes to neutrino scattering. Also, the neutrino may have an anapole moment, whose effect on neutrino scattering by a target is similar to the effect of the neutrino charge radius (see Ref. [1] for a detailed discussion of this issue).

In the SM, the electric neutrality of the neutrino is due to the cancellation of gauge anomalies in the case of electroweak interaction. However, if we consider theories featuring massive right-handed Dirac neutrinos, which are singlets of the $SU(2)$ weak-isospin group and which have a nonzero hypercharge, scenarios in which the neutrino has a nonzero electric charge become possible [37]. As a result, the cancellation of gauge anomalies requires the respective shift of charges of charged leptons and quarks and, hence, of electrons, protons, and neutrons. It follows that the neutrino charge should be sufficiently small for the electric neutrality of matter to remain unaltered. This yields the constraint [38]

$$|e_{ee}| \lesssim 3 \times 10^{-21} e_0. \quad (11)$$

Even if the electric charge of the neutrino is zero, the charge form factor $f_Q^{fi}(q^2)$ may carry nontrivial information about neutrino electric properties—namely, about the neutrino charge radius. The calculation of the neutrino charge radius within the SM yields diagonal in the

flavour basis results [4–6]

$$\langle r_{\ell\ell}^2 \rangle_{SM} = \frac{G_F}{4\sqrt{2}\pi^2} \left[3 - 2 \log \frac{m_\ell^2}{m_W^2} \right], \quad (12)$$

where m_W and m_ℓ are the W -boson and charged lepton ($\ell = e, \mu, \tau$) masses, respectively. From Eq. (12), one can obtain the following numerical estimates:

$$\begin{aligned} \langle r_{ee}^2 \rangle_{SM} &= 4.1 \times 10^{-33} \text{ cm}^2, \\ \langle r_{\mu\mu}^2 \rangle_{SM} &= 2.4 \times 10^{-33} \text{ cm}^2, \\ \langle r_{\tau\tau}^2 \rangle_{SM} &= 1.5 \times 10^{-33} \text{ cm}^2, \end{aligned} \quad (13)$$

These values are only one order of magnitude less than the current experimental limits: $|\langle r_{\ell\ell}^2 \rangle| \lesssim 10^{-32} \text{ cm}^2$ [34]. Also, as mentioned in Ref. [5], the SM predicts nonzero values for the neutrino diagonal in the flavour basis anapole moments. According to the vertex decomposition (7) it is simply

$$a_{\ell\ell}^{SM} = -\frac{1}{6} \langle r_{\ell\ell}^2 \rangle_{SM}. \quad (14)$$

B. Nucleon EM and weak neutral form factors

In describing neutrino-nucleon scattering, we use the nucleon EM vertex function in the standard form [33, 39] [setting $m_f = m_i = m_N$ in Eq. (6), where m_N is the nucleon mass]

$$\Lambda_\mu^{(\text{EM};N)}(q) = \gamma_\mu F_Q^N(q^2) - \frac{i}{2m_N} \sigma_{\mu\nu} q^\nu F_M^N(q^2) + \frac{1}{2m_N} \sigma_{\mu\nu} q^\nu \gamma_5 F_E^N(q^2) - (q^2 \gamma_\mu - q_\mu \not{q}) \gamma_5 \frac{F_A^N(q^2)}{m_N^2}. \quad (15)$$

Here $F_{Q,M,E,A}$ are, respectively, charge, magnetic, electric, and anapole form factors for the proton ($N = p$) and the neutron ($N = n$).

In the case of the weak neutral current, we disregard second-class currents, which violate isotopic invariance of strong interaction—that is, we set $f_1 = f_6 = 0$ in Eq. (3). As a result, we obtain [40, 41]

$$\Lambda_\mu^{(\text{NC};N)}(q) = \gamma_\mu F_1^N(q^2) - \frac{i}{2m_N} \sigma_{\mu\nu} q^\nu F_2^N(q^2) - \gamma_\mu \gamma_5 G_A^N(q^2) + \frac{1}{m_N} G_P^N(q^2) q^\mu \gamma_5, \quad (16)$$

where F_1^N , F_2^N , G_A^N , and G_P^N are referred to as, respectively, the nucleon Dirac, Pauli, axial, and pseudoscalar weak neutral form factors. Below, we omit the pseudoscalar form factor G_P^N , since its contribution to the neutrino-nucleon cross section vanishes in the limit of zero neutrino mass.

Restricting ourselves, in the description of the internal structure of nucleons, to the u , d and s light quarks, for which $SU(3)$ flavor symmetry holds approximately, and employing the hypotheses of vector current conservation and partial axial-current conservation, we can relate nucleon weak neutral currents to nucleon EM currents. This entails relations between the respective form factors [40, 42] (here, we restrict ourselves to the charge and magnetic form factors in the case of the EM current). Specifically, we have

$$\begin{aligned}
F_{1,2}^p(q^2) &= \left(\frac{1}{2} - 2 \sin^2 \theta_W \right) F_{Q,M}^p - \frac{3}{2} F_{Q,M}^n - \frac{1}{2} F_{1,2}^S, \\
F_{1,2}^n(q^2) &= \left(\frac{1}{2} - 2 \sin^2 \theta_W \right) F_{Q,M}^n - \frac{3}{2} F_{Q,M}^p - \frac{1}{2} F_{1,2}^S, \\
G_A^p(q^2) &= \frac{1}{2} G_A(q^2) - \frac{1}{2} G_A^S(q^2), \\
G_A^n(q^2) &= -\frac{1}{2} G_A(q^2) - \frac{1}{2} G_A^S(q^2),
\end{aligned} \tag{17}$$

where G_A is the axial form factor, while $F_{1,2}^S$ and G_A^S are the strange form factors for the nucleon.

C. Parametrization of nucleon form factors

In the literature, the q^2 dependence of the nucleon form factors is frequently described in the dipole approximation. However, the parametrization of the nucleon form factors in the dipole approximation is not always sufficient for performing a detailed analysis of experimental data on lepton-nucleon scattering. For this reason, we make use here of the more accurate approach developed in Refs. [41, 42].

We introduce the Sachs EM form factors $G_{E,M}^N$,

$$F_Q^N(q^2) = \frac{G_E^N(q^2) - \frac{q^2}{4m_N^2} G_M^N(q^2)}{1 - \frac{q^2}{4m_N^2}}, \quad F_M^N(q^2) = \frac{G_M^N(q^2) - G_E^N(q^2)}{1 - \frac{q^2}{4m_N^2}}, \tag{18}$$

which are parametrized as

$$\begin{aligned}
\frac{G_M^N(q^2)}{\mu_N} &= \frac{1 - \frac{q^2}{4m_N^2} a_M^N}{1 - \frac{q^2}{4m_N^2} b_{M1}^N + \left(\frac{q^2}{4m_N^2}\right)^2 b_{M2}^N - \left(\frac{q^2}{4m_N^2}\right)^3 b_{M3}^N}, \\
G_E^p(q^2) &= \frac{1 - \frac{q^2}{4m_N^2} a_E^p}{1 - \frac{q^2}{4m_N^2} b_{E1}^p + \left(\frac{q^2}{4m_N^2}\right)^2 b_{E2}^p - \left(\frac{q^2}{4m_N^2}\right)^3 b_{E3}^p}, \\
G_E^m(q^2) &= \frac{-\frac{q^2}{4m_N^2} \lambda_1}{1 - \frac{q^2}{4m_N^2} \lambda_2} \left(1 - \frac{q^2}{M_V^2}\right)^{-2},
\end{aligned} \tag{19}$$

where μ_N is the nucleon magnetic moment in nuclear magneton units. For the axial form factor, we use the parametrization

$$G_A(q^2) = g_A \left(1 - \frac{q^2}{M_A^2}\right)^{-2}. \tag{20}$$

We now present the numerical values of all of the parameters used here [41]:

$$\begin{aligned}
m_N &= 938 \text{ MeV}, & \mu_p &= 2.793, & \mu_n &= -1.913, \\
M_V &= 843 \text{ MeV}, & g_A &= 1.267, & M_A &= 1049 \text{ MeV}, \\
a_E^p &= -0.19, & b_{E1}^p &= 11.12, & b_{E2}^p &= 15.16, & b_{E3}^p &= 21.25, \\
a_M^p &= 1.09, & b_{M1}^p &= 12.31, & b_{M2}^p &= 25.57, & b_{M3}^p &= 30.61, \\
& & \lambda_1 &= 1.68, & \lambda_2 &= 3.63, \\
a_M^n &= 8.28, & b_{M1}^n &= 21.3, & b_{M2}^n &= 77, & b_{M3}^n &= 238.
\end{aligned} \tag{21}$$

The strange form factors are parameterized as [43]

$$\begin{aligned}
F_1^S(q^2) &= \frac{\frac{q^2}{6} \langle r_S^2 \rangle}{\left(1 - \frac{q^2}{4m_N^2}\right)} \left(1 - \frac{q^2}{M_V^2}\right)^{-2}, \\
F_2^S(q^2) &= \frac{\mu_S}{\left(1 - \frac{q^2}{4m_N^2}\right)} \left(1 - \frac{q^2}{M_V^2}\right)^{-2}, \\
F_A^S(q^2) &= g_A^S \left(1 - \frac{q^2}{M_A^2}\right)^{-2},
\end{aligned} \tag{22}$$

where $\langle r_S^2 \rangle$ is the strange nucleon radius, μ_S is the strange nucleon magnetic moment, and g_A^S is the strange contribution to the nucleon spin. Measurements of strange vector form factors $F_{1,2}^S$ in parity-violating electron scattering indicate their values close to zero [44]. Therefore, in this work, following Ref. [45], we neglect the contributions of strangeness, i.e.,

it is assumed that $F_{1,2}^S = 0$. However, we take into account the strange contribution to the weak axial form factor. We consider $0.2 \geq g_A^S \geq -0.2$, which almost completely covers the experimental values of g_A^S (see, for example, Ref. [45]). In the present study, we will compare the scattering cross sections calculated with and without allowance for the above strange form factors.

III. CROSS SECTIONS FOR ELASTIC NEUTRINO-NUCLEON SCATTERING

We consider the process where an ultrarelativistic neutrino with 4-momentum $k^\mu = (E_\nu, \mathbf{k})$ originates from a source (reactor, accelerator, the Sun, etc.) and elastically scatters on a nucleon in a detector at energy-momentum transfer $q = (T, \mathbf{q})$. If the neutrino has nonzero magnetic moment, its spin-flavor oscillations may take place due to interactions with a magnetic field in the source and with interstellar and/or intergalactic magnetic fields. In the most general case, the neutrino state in the detector can be mixed both in flavour/mass space and in spin space. We can describe the neutrino state before scattering by a statistical operator acting in the Hilbert space of neutrino mass and spin states as

$$\rho_{ij} = \alpha_{ij} u_{k,-}^{(\nu_i)} \bar{u}_{k,-}^{(\nu_j)} + \kappa_{ij} u_{k,-}^{(\nu_i)} \bar{u}_{k,+}^{(\nu_j)} + \kappa_{ji}^* u_{k,+}^{(\nu_i)} \bar{u}_{k,-}^{(\nu_j)} + \beta_{ij} u_{k,+}^{(\nu_i)} \bar{u}_{k,+}^{(\nu_j)}, \quad (23)$$

where α, β are hermitian matrices, $u_{k,\pm}^{(\nu_i)}$ is the bispinor amplitude of the massive neutrino state $|\nu_i\rangle$ with 4-momentum k and positive (+) or negative (-) helicity, and in the Weyl representation it has the form

$$u_{k,\pm}^{(\nu_i)} = \begin{pmatrix} \sqrt{(k \cdot \sigma)} \xi_\pm \\ \sqrt{(k \cdot \bar{\sigma})} \xi_\pm \end{pmatrix} = \begin{pmatrix} \sqrt{E_\nu(m_i) \mp |\mathbf{k}|} \xi_\pm \\ \sqrt{E_\nu(m_i) \pm |\mathbf{k}|} \xi_\pm \end{pmatrix}. \quad (24)$$

Here ξ_\pm are helicity 2-component eigenspinors, $(\mathbf{k} \cdot \boldsymbol{\sigma}) \xi_\pm = \pm |\mathbf{k}| \xi_\pm$. In the ultrarelativistic limit these bispinor amplitudes are also the chirality eigenstates

$$u_{k,+}^{(\nu_i)} = \sqrt{2E_\nu} \begin{pmatrix} 0 \\ \xi_+ \end{pmatrix}, \quad u_{k,-}^{(\nu_j)} = \sqrt{2E_\nu} \begin{pmatrix} \xi_- \\ 0 \end{pmatrix}, \quad (25)$$

and $E_\nu = |\mathbf{k}|$. Substituting the explicit form (25) in Eq. (23), we can rewrite the density matrix as a generalization of the ultrarelativistic spin density matrix for a Dirac particle:

$$\rho_{ij} = \frac{1}{2} \not{k} \left(\tilde{\rho}_{ij} - \zeta_{ij}^\parallel \gamma_5 + (\boldsymbol{\zeta}_{ij}^\perp \cdot \boldsymbol{\gamma}_\perp) \gamma_5 \right), \quad (26)$$

where $\tilde{\rho}_{ij} = \frac{1}{2E_\nu} \text{tr}(\rho_{ij}\gamma^0) = \alpha_{ij} + \beta_{ij}$ is a reduced density matrix in the neutrino mass space. $\frac{1}{2}\zeta_{ij}^{\parallel} = \frac{1}{2}(\beta_{ij} - \alpha_{ij})$ and, with $\{\mathbf{e}_x, \mathbf{e}_y, \mathbf{k}/E_\nu\}$ forming a 3-vector basis, $\zeta_{ij}^{\perp} = \zeta_{ij}^x \mathbf{e}_x + \zeta_{ij}^y \mathbf{e}_y = (\kappa_{ij} + \kappa_{ji}^*) \mathbf{e}_x - i(\kappa_{ij} - \kappa_{ji}^*) \mathbf{e}_y$ are the matrices of longitudinal (\parallel) and transverse (\perp) components, with respect to the neutrino momentum k , corresponding to the diagonal ($i = j$) and transition ($i \neq j$) values of the spin operator Σ averaged over spin states of the neutrino in its rest frame. If there is a state with zero neutrino mass then the diagonal and transition ζ^{\perp} components involving this state vanish. Thus, the density matrix (26) contains the information about all the neutrino spin components, so that, for example, $\frac{1}{2E_\nu} \text{tr}(\rho_{ij}\gamma^0 \frac{1}{2}\Sigma) = \frac{1}{2}\zeta_{ij}^{\parallel} \frac{\mathbf{k}}{E_\nu}$ are the values of the spin operator averaged over neutrino spin states in the lab frame (there is only longitudinal part, as it should be for the ultrarelativistic limit). Also we note that the density matrix (23) can be determined taking into account that in the ultrarelativistic limit the components of the spin-flavour density matrix in the mass basis typically employed in neutrino oscillation calculations are related to the components $\frac{1}{4E_\nu^2} (u_{k,r'}^{(\nu_i)})^\dagger \rho_{ij} \gamma^0 u_{k,r}^{(\nu_j)}$. Such a density matrix acting on the column vectors in the basis of neutrino states $\{(\nu_1^R, \nu_2^R, \nu_3^R), (\nu_1^L, \nu_2^L, \nu_3^L)\}$ can be presented as

$$\rho = \begin{pmatrix} \beta & \kappa^\dagger \\ \kappa & \alpha \end{pmatrix} = \frac{1}{2} \begin{pmatrix} \tilde{\rho} + \zeta^{\parallel} & \zeta^x - i\zeta^y \\ \zeta^x + i\zeta^y & \tilde{\rho} + \zeta^{\parallel} \end{pmatrix} = \frac{1}{2} \left(\tilde{\rho} \mathbb{1} + (\zeta \cdot \hat{\sigma}) \right), \quad (27)$$

where $\mathbb{1}$ and the Pauli matrices $\hat{\sigma}$ are assumed to be the block matrices with their components being matrices acting on the mass states.

The matrix element of the transition $\nu_i + N \rightarrow \nu_n + N$ due to the weak interaction is given by

$$\mathcal{M}^{(w)} = -\frac{G_F}{\sqrt{2}} \bar{u}_{k',r'}^{(\nu_n)} \gamma^\mu (1 - \gamma^5) \delta^{ni} u_{k,r}^{(\nu_i)} J_\mu^{(NC)}(q), \quad (28)$$

where $J_\lambda^{(NC)}(q)$ is the neutral weak nucleon current. The matrix element due to the EM interaction is given by

$$\mathcal{M}^{(\gamma)} = \frac{4\pi\alpha}{q^2} \bar{u}_{k',r'}^{(\nu_n)} \Lambda_\mu^{(EM;\nu)ni}(q) u_{k,r}^{(\nu_i)} J^{(EM)\mu}(q), \quad (29)$$

where $J_\mu^{(EM)}(q)$ is the EM nucleon current. Assuming the target nucleon to be free, these

nucleon transition currents can be parameterized as follows:

$$\begin{aligned}
J_\mu^{(NC)}(q) &= \bar{u}_{p',s'}^{(N)} \Lambda_\mu^{(NC;N)}(-q) u_{p,s}^{(N)} \\
&= F_1^N(q) J_\mu^V(q) - G_A^N(q) J_\mu^A(q) + \frac{i}{2m_N} F_2^N(q) J_\mu^M(q), \\
J_\mu^{(EM)}(q) &= \bar{u}_{p',s'}^{(N)} \Lambda_\mu^{(EM;N)}(-q) u_{p,s}^{(N)} \\
&= F_Q(q)^N J_\mu^V(q) - (\delta_\mu^\lambda q^2 - q^\lambda q_\mu) \frac{F_A^N(q)}{m_N^2} J_\mu^A(q) + \frac{i}{2m_N} F_M^N(q) J_\mu^M(q) - \frac{F_E^N(q)}{2m_N} J_\mu^E(q),
\end{aligned} \tag{30}$$

where

$$\begin{aligned}
J_\mu^V(q) &= \bar{u}_{p',s'}^{(N)} \gamma_\mu u_{p,s}^{(N)}, & J_\mu^A(q) &= \bar{u}_{p',s'}^{(N)} \gamma_\mu \gamma_5 u_{p,s}^{(N)}, \\
J_\mu^M(q) &= \bar{u}_{p',s'}^{(N)} \sigma_{\mu\alpha} q^\alpha u_{p,s}^{(N)} & J_\mu^E(q) &= \bar{u}_{p',s'}^{(N)} \sigma_{\mu\alpha} q^\alpha \gamma_5 u_{p,s}^{(N)},
\end{aligned} \tag{31}$$

with $u_{p,s}^{(N)}$ being the bispinor amplitude of the nucleon with four-momentum p and spin s .

Since we are interested in the scattering of ultrarelativistic neutrinos, we disregard the neutrino mass in our calculations of the cross section. In the lab frame with z -axis directed along the incident neutrino momentum we calculate the angular differential cross section

$$\frac{d\sigma}{d\Omega} = \frac{d^2\sigma}{\sin\theta d\theta d\varphi} = \frac{|\mathcal{M}|^2 t^2}{64\pi^2 (s - m_N^2)^2 m_N^2} \left(1 - \frac{4m_N^2}{t}\right)^{3/2} \tag{32}$$

in terms of the Mandelstam variables

$$s = (k + p)^2 = m_N^2 + 2E_\nu m_N, \quad t = (k - k')^2 = -\frac{4m_N^2 E_\nu^2 \cos^2 \theta}{(E_\nu + m_N)^2 - E_\nu^2 \cos^2 \theta}$$

as a function of the polar (θ) and azimuthal (φ) angles of the recoil nucleon. Also, averaging over initial and summing over final spin polarizations of the nucleon ($\frac{1}{2} \sum_{s',s}$) and summing over final neutrino polarisations ($\sum_{r'}$) and final neutrino mass states (\sum_f) are assumed. The absolute matrix element squared for the neutrino initial and final states ρ_{ij} and $\rho_{n'n}^f$ has the following structure:

$$|\mathcal{M}|^2 = \frac{G_F^2}{2} \sum_{i,j,n,n'=1}^3 \frac{1}{2} \sum_{s's} \sum_{r'} \sum_f \text{tr} \{ \rho_{n'n}^f \mathcal{O}_{ni}^{s's} \rho_{ij} \gamma^0 (\mathcal{O}_{n'j}^{s's})^\dagger \gamma^0 \}, \tag{33}$$

where $\mathcal{O}_{ni}^{s's}$ describes interactions with the nucleon neutral weak and EM currents

$$\mathcal{O}_{ni}^{s's} = \delta_{ni} \gamma^\mu (1 - \gamma_5) J_\mu^{s's(NC)}(q) - \frac{4\sqrt{2}\pi\alpha}{G_F^2 q^2} \Lambda_{ni}^{(EM;\nu)\mu}(q) J_\mu^{s's(EM)}(q). \tag{34}$$

In the calculation, we take into account that $\sum_{r'} \sum_f \rho_{n'n}^f = \delta_{n'n} \not{k}'$. Therefore, the cross section can be split into the following parts:

$$\frac{d\sigma}{d\Omega} = \frac{d\sigma^L}{d\Omega} + \frac{d\sigma^R}{d\Omega} + \frac{d\sigma^\perp}{d\Omega}, \tag{35}$$

where $\frac{d\sigma^K}{d\Omega}$ are cross sections with projection of the initial neutrino state on the left ($K = L$) and right ($K = R$) helicity states, respectively. Both of them can be divided into helicity-preserving and helicity-flipping components (to avoid encumbering the presentation, we omit the argument $q^2 = t$ in the expressions for the form factors); that is,

$$\begin{aligned}
\frac{d\sigma^K}{d\Omega} &= \frac{d\sigma_{\text{hp}}^K}{d\Omega} + \frac{d\sigma_{\text{hf}}^K}{d\Omega}, \\
\frac{d\sigma_{\text{hp}}^K}{d\Omega} &= \frac{G_F^2 t^2 (s - m_N^2)}{16\pi^2 m_N^2 (s + m_N^2)} \left(1 - \frac{4m_N^2}{t}\right)^{3/2} \\
&\quad \times \left[2 \left(1 + \frac{st}{(s - m_N^2)^2}\right) \left(C_V^K + C_A^K - \frac{t}{4m_N^2} (C_M^K + C_E^K)\right) \right. \\
&\quad - \frac{4m_N^2 t}{(s - m_N^2)^2} \left(C_A^K - \frac{t}{4m_N^2} C_M^K\right) + \frac{t^2}{(s - m_N^2)^2} (C_V^K + C_A^K - 2\text{Re } C_{V\&M}^K) \\
&\quad \left. \pm \frac{2t}{s - m_N^2} \left(2 + \frac{t}{s - m_N^2}\right) \text{Re} (C_{V\&A}^K - C_{A\&M}^K) \right], \\
\frac{d\sigma_{\text{hf}}^K}{d\Omega} &= \frac{\alpha^2 t^2 (s - m_N^2)}{8m_e^2 m_N^2 (s + m_N^2)} \left(1 - \frac{4m_N^2}{t}\right)^{3/2} |\mu_\nu^K|^2 \left[-\frac{2m_N}{t} \left(1 + \frac{t}{s - m_N^2}\right) (F_Q^N)^2 \right. \\
&\quad - \frac{2t}{m_N^3} \left(1 + \frac{st}{(s - m_N^2)^2}\right) (F_A^N)^2 + \frac{m_N t}{(s - m_N^2)^2} F_Q^N F_M^N \\
&\quad \left. + \frac{1}{8m_N} \left(4 + \frac{4st + t^2}{(s - m_N^2)^2}\right) (F_M^N)^2 + \frac{1}{8m_N} \left(2 + \frac{t}{s - m_N^2}\right)^2 (F_E^N)^2 \right],
\end{aligned} \tag{36}$$

where $+$ ($-$) stands for $K = L$ ($K = R$) and [46]

$$\begin{aligned}
C_V^K &= \text{Tr} \left[(-F_1^N \delta_L^K + F_Q^N Q^K)^2 \rho^K \right], & C_A^K &= \text{Tr} \left[\left(\delta_L^K G_A^N - \frac{t F_A^N Q^K}{m_N^2} \right)^2 \rho^K \right], \\
C_{V\&A}^K &= \text{Tr} \left[\left(\delta_L^K G_A^N - \frac{t F_A^N Q^K}{m_N^2} \right) (-F_1^N \delta_L^K + F_Q^N Q^K) \rho^K \right], & C_M^K &= \text{Tr} \left[(\delta_L^K F_2^N - F_M^N Q^K)^2 \rho^K \right], \\
C_{V\&M}^K &= \text{Tr} \left[(\delta_L^K F_2^N - F_M^N Q^K) (-F_1^N \delta_L^K + F_Q^N Q^K) \rho^K \right], & C_E^K &= \text{Tr} \left[(F_E Q^K)^2 \rho^K \right], \\
C_{A\&M}^K &= \text{Tr} \left[(\delta_L^K F_2^N - F_M^N Q^K) \left(\delta_L^K G_A^N - \frac{t F_A^N Q^K}{m_N^2} \right) \rho^K \right], \\
\rho^{L,R} &= \frac{1}{2} (\tilde{\rho} \mp \zeta^\parallel), & Q^{L,R} &= \frac{2\sqrt{2}\pi\alpha}{G_F t} (f^Q \mp t f^A), & |\mu_\nu^{L,R}|^2 &= \text{Tr} \left[(f^M \pm i f^E) (f^M \mp i f^E) \rho^{L,R} \right].
\end{aligned} \tag{37}$$

The cross section $\frac{d\sigma^\perp}{d\Omega}$ describes the contribution from the interference of the helicity states and depends on the transverse neutrino spin components ζ_{ij}^x and ζ_{ij}^y written in terms of

$\kappa_{ij} = \frac{1}{2}(\zeta_{ij}^x + i\zeta_{ij}^y)$ [see the text after Eq. (26)]

$$\begin{aligned}
\frac{d\sigma^\perp}{d\Omega} = & \frac{\sqrt{2}G_F\alpha(s - m_N^2)(4m_N^2 - t)^{3/2}}{8\pi m_e m_N^2(s + m_N^2)} \sqrt{1 + \frac{st}{(s - m_N^2)^2}} \left\{ \frac{2t}{s - m_N^2} \frac{tF_A^N}{m_N^2} (F_Q^N + F_M^N) C_{\mu\nu,Q}^+ \right. \\
& + C_{\mu\nu,Z^0}^\perp \left[\left(2 + \frac{t}{s - m_N^2} \right) \left(F_1^N F_Q^N + \frac{tF_A^N}{m_N^2} G_A^N - t \frac{F_2^N F_M^N}{4m_N^2} \right) \right. \\
& \left. \left. - \frac{t}{s - m_N^2} \left(\frac{tF_A^N}{m_N^2} (F_1^N + F_2^N) + G_A^N (F_Q^N + F_M^N) \right) \right] \right. \\
& \left. - \left(2 + \frac{t}{s - m_N^2} \right) \left((F_Q^N)^2 + \left(\frac{tF_A^N}{m_N^2} \right)^2 - t \left(\frac{F_M^N}{2m_N} \right)^2 - t \left(\frac{F_E^N}{2m_N} \right)^2 \right) C_{\mu\nu,Q}^- \right\}, \tag{38}
\end{aligned}$$

where

$$\begin{aligned}
C_{\mu\nu,Z^0}^\perp &= \text{Re Tr} \left[(f^M + if^E) \kappa^\dagger e^{i\varphi} \right], \\
C_{\mu\nu,Q}^\pm &= \text{Re Tr} \left[[Q^L (f^M + if^E) \pm (f^M + if^E) Q^R] \kappa^\dagger e^{i\varphi} \right]. \tag{39}
\end{aligned}$$

It is important to note that the cross sections $\frac{d\sigma^{L,R}}{d\Omega}$ depend only on the polar angle θ and are independent of the transverse neutrino polarization components. Also, only the EM interaction contributes to the cross section for right-handed neutrinos ($K = R$). The cross section $\frac{d\sigma^\perp}{d\Omega}$ depends on both the polar and azimuthal angles of the recoil nucleon and involves the terms due to the interference between the weak and EM interactions.

IV. NUMERICAL RESULTS

Obviously, manifestations of neutrino EM properties should be much more pronounced in neutrino-proton rather than in neutrino-neutron scattering. In order to illustrate the characteristic effects of these properties, we present below the results obtained by numerically calculating the differential cross section for elastic neutrino-proton scattering.

The calculations have been made not only for the cross section $\frac{d\sigma}{d\Omega} = \frac{d^2\sigma}{\sin\theta d\theta d\varphi}$ given by Eqs. (35)-(39), but also for the cross section $\frac{d\sigma}{dT}$, which is differential with respect to the energy transfer T and which determines the shape of the nucleon recoil spectrum. The cross sections are related to each other in accordance with

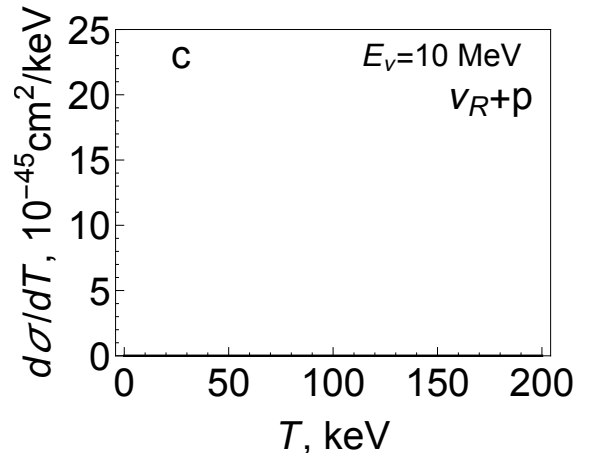
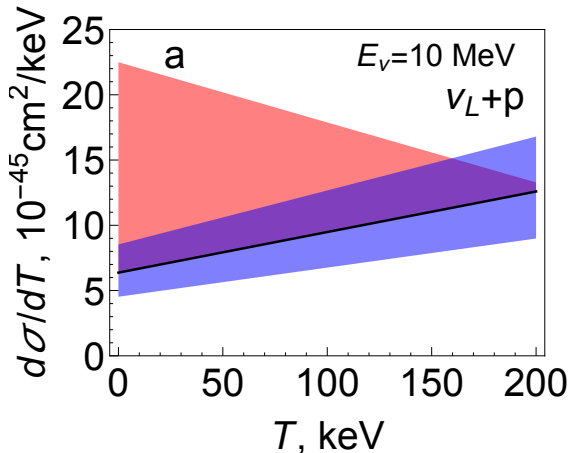
$$\cos\theta = \sqrt{\frac{T}{T + 2m_N} \frac{E_\nu + m_N}{E_\nu}}, \quad \frac{d\sigma}{dT} = \frac{m_N(E_\nu + m_N)}{E_\nu T (T + 2m_N)^{3/2}} \int_0^{2\pi} \frac{d\sigma}{d\Omega} d\varphi. \tag{40}$$

A. Neutrino charge radii

First, we present numerical calculations for cross sections differential with respect to the energy transfer T with and without allowance for the neutrino charge radii. The calculations are performed for neutrino energies typical for supernova sources. It is generally believed that, due to the neutrino flavor oscillations and their decoherence on a large source-detector base, the supernova neutrino should arrive at the detector as an incoherent mixture of three flavor states ($\ell = e, \mu, \tau$). For each neutrino flavor three different spin states are considered: the arriving neutrino can be either left-handed, right-handed, or fully unpolarized. The SM results are obtained both with and without taking into account the strange contribution to the proton form factors, which was treated according to the approach outlined in Sec. II C. In the case of the diagonal neutrino charge radii, we used the SM values (13). However, their effect is so small that the corresponding results are visually indistinguishable from the results without them. Therefore, fig. 1 shows the effect of the neutrino transition charge radii. For the latter we employed the values (in cm^2) in the range which is consistent with the current experimental constraints [27, 29, 34]:

$$0 \leq |\langle r_{e\mu}^2 \rangle|, |\langle r_{e\tau}^2 \rangle|, |\langle r_{\mu\tau}^2 \rangle| < 3 \times 10^{-31}. \quad (41)$$

In such a case the results do not depend on the neutrino flavour.



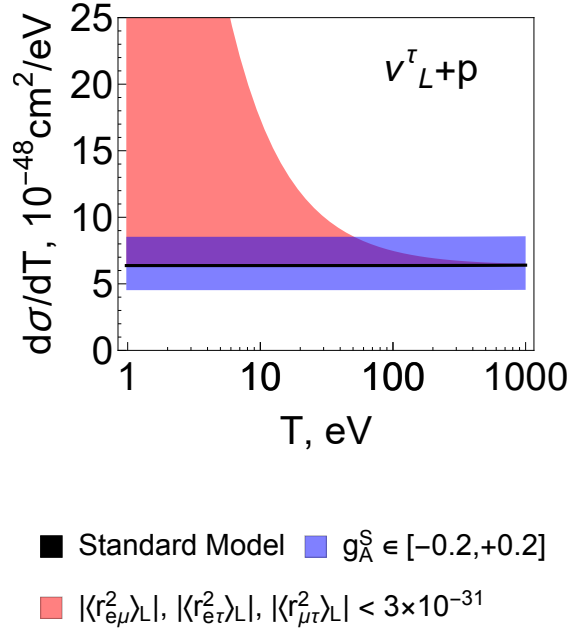


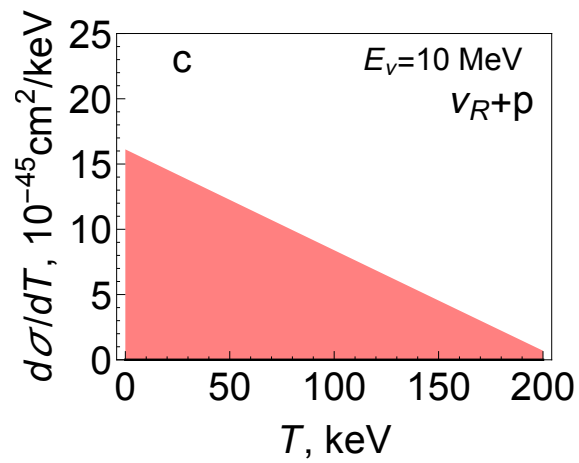
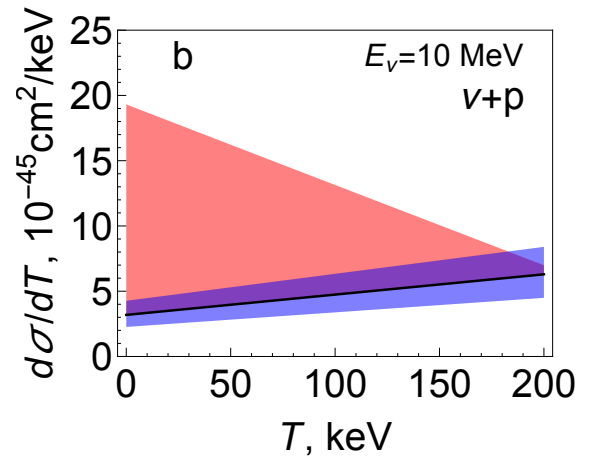
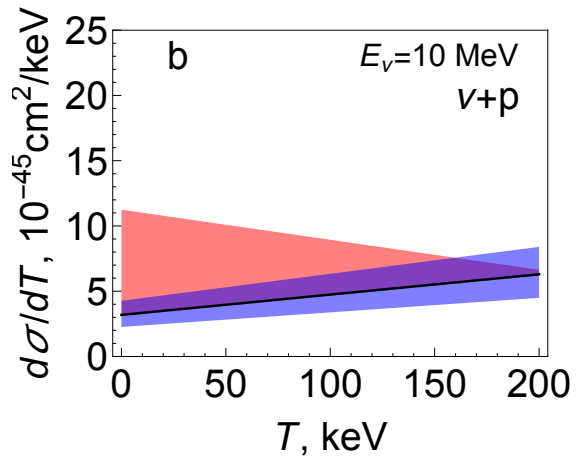
Figure 1: The effect of the neutrino transition charge radii on the differential cross section for elastic neutrino-proton scattering in the cases of different initial neutrino spin states in the detector: (a) left-handed, (b) fully unpolarized and (c) right-handed. The neutrino energy is $E_\nu = 10$ MeV, which is typical for a supernova source.

B. Neutrino anapole moments

We also examine possible contributions from neutrino anapole moments. Similarly to fig. 1, the SM predictions for diagonal anapole moments (14) bring about only minor corrections, which cannot be visually distinguished from the results without them. On the other hand, the current neutrino scattering experiments limit the effective charge radii $\langle r_{ij}^2 \rangle_L = \langle r_{ij}^2 \rangle - 6a_{ij}$, which are linear combinations of the neutrino charge radii and anapole moments. Namely, one should make the substitution $\langle r_{ij}^2 \rangle \rightarrow \langle r_{ij}^2 \rangle_L$ in Eq. (41). Therefore, when we calculate the effect of transition anapole moments while assuming zero charge radii, we obtain the results identical to those in fig. 1.

Figure 2 shows the calculations with the neutrino charge radii and anapole moments, provided the SM-like relationship (14) between them holds, i.e.,

$$a_{ij} = -\frac{1}{6}\langle r_{ij}^2 \rangle, \quad i, j = \{1, 2, 3\}. \quad (42)$$



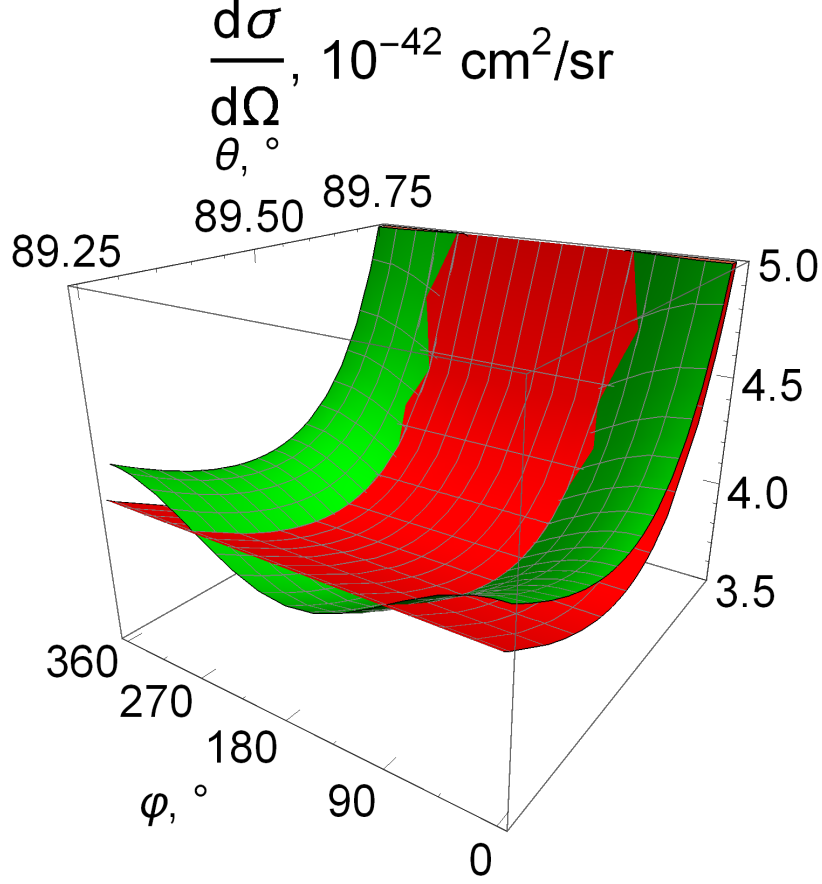


Figure 2: The same as in fig. 1, but in the case of the effective neutrino transition charge radii.

Figure 1 demonstrates that neutrino EM properties reveal themselves considerably for both left- and right-handed neutrinos, whereas fig. 2 demonstrates that the effects of charge radii and anapole moments can be distinguished. Thus, due to Eq. (42) the cross section for left-handed neutrinos depends on the linear combination $\langle r_{ij}^2 \rangle_L = \langle r_{ij}^2 \rangle - 6a_{ij} = 2\langle r_{ij}^2 \rangle$ and exhibits the maximum EM effect, while for right-handed neutrinos the cross section depends on the linear combination $\langle r_{ij}^2 \rangle_R = \langle r_{ij}^2 \rangle + 6a_{ij} = 0$ and there is no EM effect at all. At the same time, it should be noted that in the general case of beyond-SM theories the relation (42) does not necessarily hold and the neutrino charge radius and anapole moment can arise as independent EM characteristics.

C. Neutrino magnetic moments

Figure 3 shows the effects of the neutrino magnetic moments (in units of μ_B) lying in the ranges [47]

$$|\mu_{ee}| < 1.5 \times 10^{-11}, \quad |\mu_{\mu\mu}| < 2.3 \times 10^{-11}, \quad |\mu_{\tau\tau}| < 2.1 \times 10^{-11}, \quad (43)$$

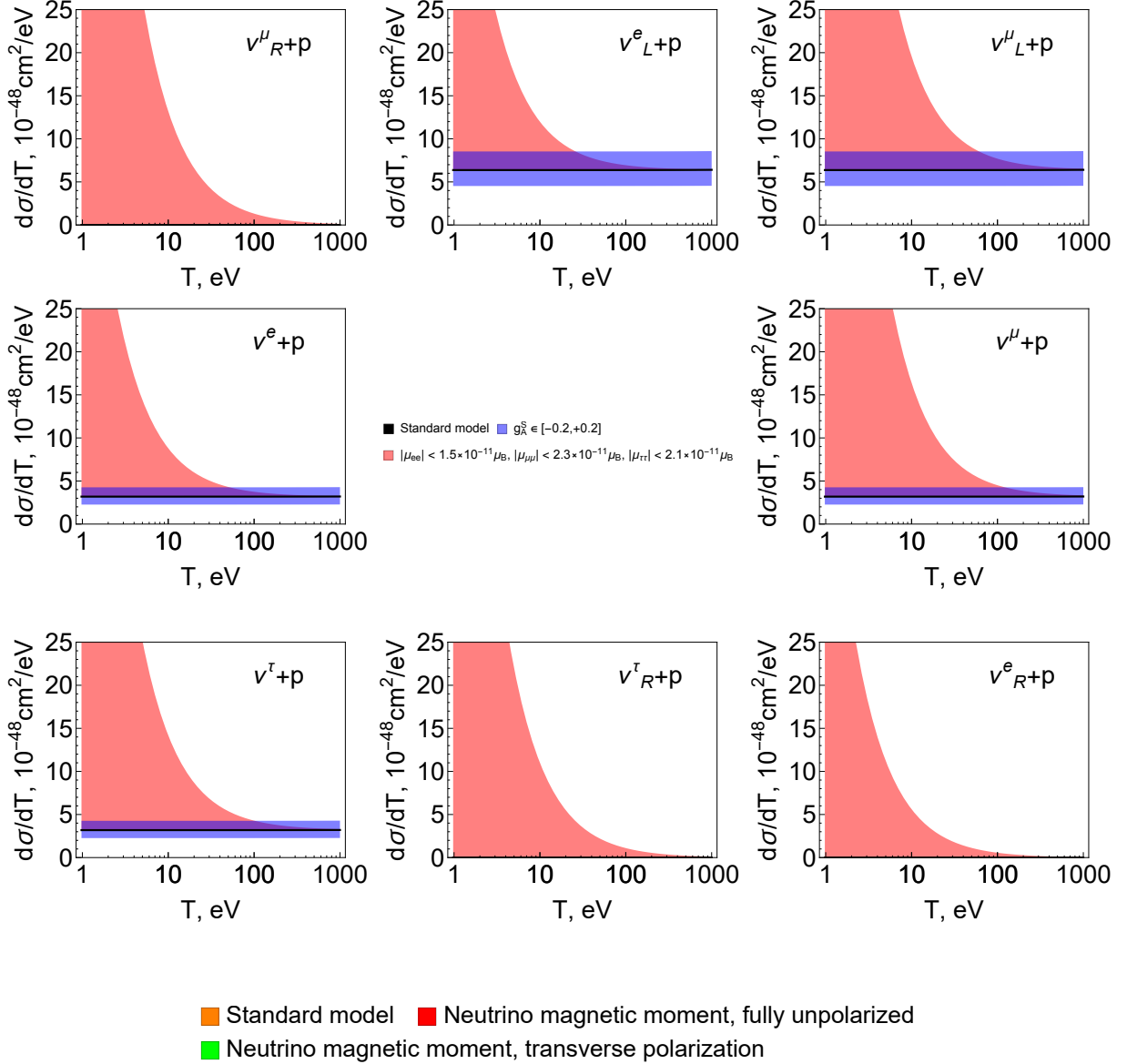


Figure 3: The differential cross section for elastic neutrino-proton scattering in the cases of different initial neutrino states in the detector. Top, middle and bottom rows correspond to the electron, muon and tau flavors, respectively. Left, middle and right columns correspond to left-handed, fully unpolarized and right-handed neutrinos, respectively.

which also reflect typical values of upper limits obtained for the neutrino magnetic moment from various neutrino scattering experiments [27–29, 34, 48]. Since for a nonzero neutrino magnetic moment the cross section $\frac{d\sigma}{dT}$ is singular when $T \rightarrow 0$, we show the region of low energy transfers, $T \ll E_\nu$. It should be noted that in such kinematical regime the cross section is practically independent of E_ν .

D. Neutrino transverse spin polarization

Figure 4 illustrates the effect of the neutrino transverse spin polarization on the cross section differential with respect to the solid angle of the recoil proton. Let us note that only when there is a transverse component of the neutrino spin polarization the cross section depends on the azimuthal angle of the recoil nucleon. We assume the initial neutrino to be fully transversely polarized relative to the initial neutrino momentum and compare this case with that when the neutrino is fully unpolarized. As follows from Eq. (38), the contribution from the neutrino transverse spin polarization to the cross section is proportional to the neutrino magnetic and/or electric dipole moments, so that it completely vanishes if they have zero values. The effect turns out to be on such a tiny scale that the contributions from the neutrino charge radii and anapole moments within the SM also become visible, and, moreover, they even tend to reduce the discussed effect.

■ Standard Model ■ $g_A^\lambda \in [-0.2, +0.2]$
 ■ $|\langle r_{e\mu}^2 \rangle|, |\langle r_{e\tau}^2 \rangle|, |\langle r_{\mu\tau}^2 \rangle| < 3 \times 10^{-31}$

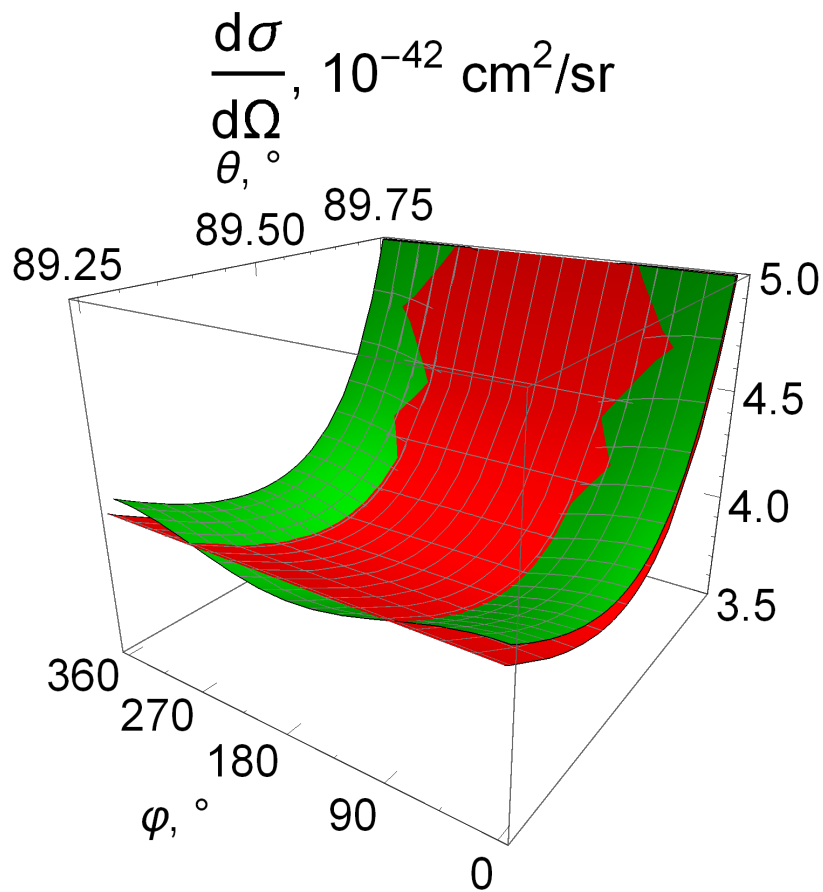
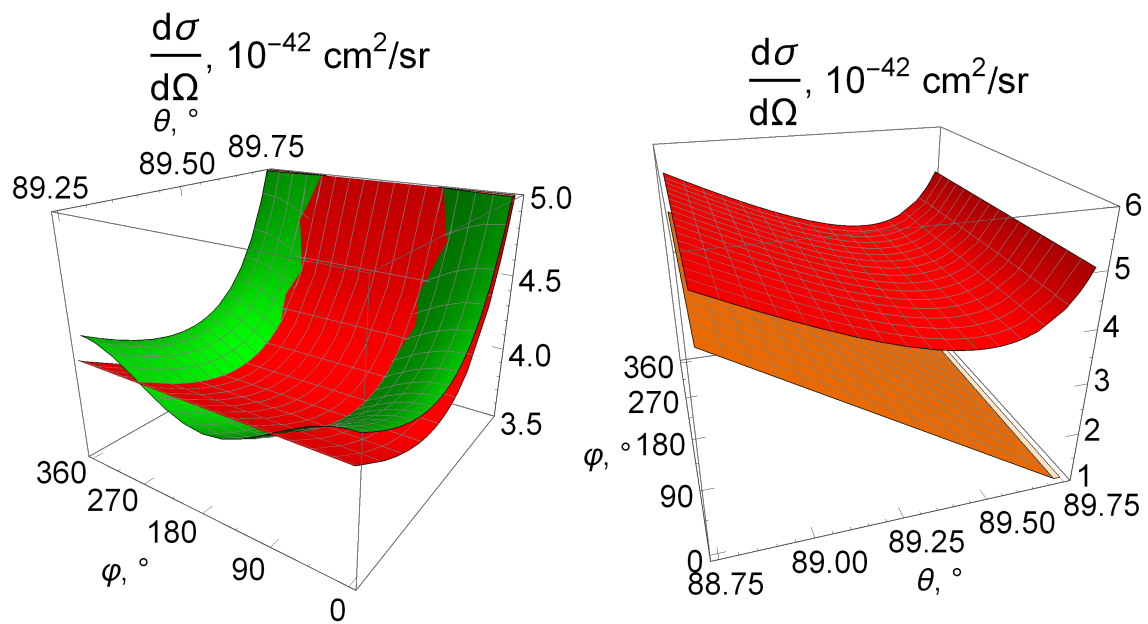


Figure 4: The angular differential cross section for elastic neutrino-proton scattering in the cases of different initial neutrino spin states in the detector. The calculations with account for neutrino magnetic moments of $10^{-11}\mu_B$ and in the case of fully unpolarized neutrinos are compared with those (a) within the SM without the neutrino charge radii and anapole moments, (b) in the case of the transverse neutrino polarization, and (c) in the case of the transverse neutrino polarization and with the account for the SM predictions for the neutrino charge radii and anapole moments.

V. SUMMARY AND CONCLUSIONS

The theory of elastic neutrino-nucleon scattering has been developed taking into account the EM interactions of massive neutrinos with arbitrary spin polarizations. The process under study proceeds via two interaction channels, namely via the Z^0 -boson and photon exchange. In either case, the nucleon form factors have been taken into account within the developed formalism. In addition, we have taken into account the mixing, oscillations and polarization of neutrinos propagating from the source to the target. We have obtained general expressions for the differential cross section for elastic neutrino-nucleon scattering and have employed them to perform numerical calculations for the scattering of supernova neutrinos on a proton target. Also, we have outlined possible manifestations of the effects of the neutrino magnetic moments, transition (in the flavor basis) charge radii and anapole moments on the cross section for left- and right-handed initial neutrino states, as well as the effects of the transverse neutrino spin polarization.

From the obtained numerical results, one can see that the neutrino EM properties can make a substantial contribution to the cross section for elastic neutrino-proton scattering. At the same time, an implementation of full-scale searches for these properties would require experimentally measuring the differential cross section over a rather wide energy-transfer range. This would permit (i) separating the effects of neutrino EM interactions from the effects associated with nucleon form factors and (ii) pinpointing neutrino EM properties that are responsible for the observed effects.

Also, our analytical and numerical calculations clearly demonstrate that the neutrino EM properties can manifest themselves both for left- and right-handed neutrinos. This means, in particular, that the fluxes of right-handed neutrinos coming to the detector should also be

taken into account. In order to point out this feature, in our numerical calculations we have considered nine different incoming neutrino states: 3 flavour states \times 3 spin states (left-handed, right-handed and fully unpolarized). In the general case, the initial neutrino state in the detector should be described by the density matrix in the space of a tensor product of flavor (or mass) and spin subspaces. The density matrix is determined by the neutrino propagation from the source to the detector, which depends on the neutrino interactions with matter and EM fields during the propagation. In such a general case, we have shown that even the transverse neutrino spin component can manifest itself in the neutrino-nucleon scattering process. On the other hand, the corresponding effect appears to be rather small. Given the structure of the derived angular differential cross section, we might expect a much larger influence of the transverse neutrino spin component in the case of nuclear targets that are much heavier than a nucleon.

Finally, the expressions for the cross sections obtained in this work carry information both about the neutrino and nucleon EM form factors. This makes it possible to apply these expressions in analyzing the results of various experiments aimed at studying neutrino interactions and oscillations in matter, detecting neutrinos from supernova explosions on the basis of elastic neutrino-proton scattering, measuring the nucleon anapole moment, and searching for the neutron electric dipole moment. Also, the results of the present study contribute to the development of a systematic approach to studying the EM properties of neutrinos in their scattering on composite targets (nuclei, atoms, and condensed media).

ACKNOWLEDGMENTS

This work is supported by the Russian Science Foundation (project No. 24-12-00084).

-
- [1] C. Giunti and A. Studenikin, *Rev. Mod. Phys.* **87**, 531 (2015), URL <https://link.aps.org/doi/10.1103/RevModPhys.87.531>.
 - [2] C. Giunti, K. A. Kouzakov, Y.-F. Li, A. V. Lokhov, A. I. Studenikin, and S. Zhou, *Ann. Phys.* **528**, 198 (2016), <https://onlinelibrary.wiley.com/doi/pdf/10.1002/andp.201500211>, URL <https://onlinelibrary.wiley.com/doi/abs/10.1002/andp.201500211>.

- [3] A. I. Studenikin and K. A. Kouzakov, *Moscow Univ. Phys. Bull.* **75**, 379 (2020), ISSN 1934-8460, URL <https://doi.org/10.3103/S0027134920050215>.
- [4] J. Bernabéu, L. G. Cabral-Rosetti, J. Papavassiliou, and J. Vidal, *Phys. Rev. D* **62**, 113012 (2000), URL <https://link.aps.org/doi/10.1103/PhysRevD.62.113012>.
- [5] J. Bernabéu, J. Papavassiliou, and J. Vidal, *Phys. Rev. Lett.* **89**, 101802 (2002), URL <https://link.aps.org/doi/10.1103/PhysRevLett.89.101802>.
J. Bernabéu, J. Papavassiliou, and J. Vidal, *Phys. Rev. Lett.* **89**, 229902(E) (2002), URL <https://link.aps.org/doi/10.1103/PhysRevLett.89.229902>.
- [6] J. Bernabéu, J. Papavassiliou, and J. Vidal, *Nucl. Phys. B* **680**, 450 (2004), ISSN 0550-3213, URL <https://www.sciencedirect.com/science/article/pii/S0550321303011003>.
- [7] K. Fujikawa and R. E. Shrock, *Phys. Rev. Lett.* **45**, 963 (1980), URL <https://link.aps.org/doi/10.1103/PhysRevLett.45.963>.
- [8] M. Drewes, *Int. J. Mod. Phys. E* **22**, 1330019 (2013), <https://doi.org/10.1142/S0218301313300191>, URL <https://doi.org/10.1142/S0218301313300191>.
- [9] L. Alvarez Ruso, A. M. Ankowski, S. Bacca, A. B. Balantekin, J. Carlson, S. Gardiner, R. Gonzalez-Jimenez, R. Gupta, T. J. Hobbs, M. Hoferichter, et al., in *contribution to Snowmass 2021* (2022), 2203.09030.
- [10] Q. Chen, Ph.D. thesis, *Theses and Dissertations—Physics and Astronomy*. 86. (2021).
- [11] O. Tomalak, P. Machado, V. Pandey, and R. Plestid, *J. High Energy Phys.* **2021**, 97 (2021), ISSN 1029-8479, URL [https://doi.org/10.1007/JHEP02\(2021\)097](https://doi.org/10.1007/JHEP02(2021)097).
- [12] O. Tomalak, Q. Chen, R. J. Hill, and K. S. McFarland, *Nat. Commun.* **13**, 5286 (2022), ISSN 2041-1723, URL <https://doi.org/10.1038/s41467-022-32974-x>.
- [13] O. Tomalak, Q. Chen, R. J. Hill, K. S. McFarland, and C. Wret, *Phys. Rev. D* **106**, 093006 (2022), URL <https://link.aps.org/doi/10.1103/PhysRevD.106.093006>.
- [14] M. A. Corona, M. Cadeddu, N. Cargioli, F. Dordei, and C. Giunti, *J. High Energy Phys.* **2024**, 271 (2024), ISSN 1029-8479, URL [https://doi.org/10.1007/JHEP05\(2024\)271](https://doi.org/10.1007/JHEP05(2024)271).
- [15] R. S. Sufian, K.-F. Liu, and D. G. Richards, *J. High Energy Phys.* **2020**, 136 (2020), ISSN 1029-8479, URL [https://doi.org/10.1007/JHEP01\(2020\)136](https://doi.org/10.1007/JHEP01(2020)136).
- [16] G. D. Megias, S. Bolognesi, M. B. Barbaro, and E. Tomasi-Gustafsson, *Phys. Rev. C* **101**, 025501 (2020), URL <https://link.aps.org/doi/10.1103/PhysRevC.101.025501>.

- [17] X. Zhang, T. J. Hobbs, and G. A. Miller, Phys. Rev. D **102**, 074026 (2020), URL <https://link.aps.org/doi/10.1103/PhysRevD.102.074026>.
- [18] J. Liang and K.-F. Liu, in *Proceedings of 37th International Symposium on Lattice Field Theory — PoS(LATTICE2019)* (Sissa Medialab, 2020), LATTICE2019, p. 046, URL <http://dx.doi.org/10.22323/1.363.0046>.
- [19] D. Z. Freedman, Phys. Rev. D **9**, 1389 (1974), URL <https://link.aps.org/doi/10.1103/PhysRevD.9.1389>.
- [20] V. B. Kopeliovich and L. L. Frankfurt, JETP Lett. **19**, 145 (1974).
- [21] D. Akimov, J. B. Albert, P. An, C. Awe, P. S. Barbeau, B. Becker, V. Belov, A. Brown, A. Bolozdynya, B. Cabrera-Palmer, et al. (COHERENT Collaboration), Science **357**, 1123 (2017), <https://www.science.org/doi/pdf/10.1126/science.aao0990>, URL <https://www.science.org/doi/abs/10.1126/science.aao0990>.
- [22] J. Yang, J. A. Hernandez, and J. Piekarewicz, Phys. Rev. C **100**, 054301 (2019), URL <https://link.aps.org/doi/10.1103/PhysRevC.100.054301>.
- [23] C. G. Payne, S. Bacca, G. Hagen, W. G. Jiang, and T. Papenbrock, Phys. Rev. C **100**, 061304(R) (2019), URL <https://link.aps.org/doi/10.1103/PhysRevC.100.061304>.
- [24] M. Hoferichter, J. Menéndez, and A. Schwenk, Phys. Rev. D **102**, 074018 (2020), URL <https://link.aps.org/doi/10.1103/PhysRevD.102.074018>.
- [25] M. Cadeddu, C. Giunti, K. A. Kouzakov, Y. F. Li, A. I. Studenikin, and Y. Y. Zhang, Phys. Rev. D **98**, 113010 (2018), URL <https://link.aps.org/doi/10.1103/PhysRevD.98.113010>.
M. Cadeddu, C. Giunti, K. A. Kouzakov, Y. F. Li, A. I. Studenikin, and Y. Y. Zhang, Phys. Rev. D **101**, 059902(E) (2020), URL <https://link.aps.org/doi/10.1103/PhysRevD.101.059902>.
- [26] O. G. Miranda, D. K. Papoulias, G. S. Garcia, O. Sanders, M. Tórtola, and J. W. F. Valle, J. High Energy Phys. **2020**, 130 (2020), ISSN 1029-8479, URL [https://doi.org/10.1007/JHEP05\(2020\)130](https://doi.org/10.1007/JHEP05(2020)130).
- [27] M. Cadeddu, F. Dordei, C. Giunti, Y. F. Li, E. Picciau, and Y. Y. Zhang, Phys. Rev. D **102**, 015030 (2020), URL <https://link.aps.org/doi/10.1103/PhysRevD.102.015030>.
- [28] H. Bonet, A. Bonhomme, C. Buck, K. Fülber, J. Hakenmüller, J. Hempfling, G. Heusser, T. Hugle, M. Lindner, W. Maneschg, et al. (C. O. N. U. S. Collaboration), Eur. Phys. J. C **82**,

- 813 (2022), ISSN 1434-6052, URL <https://doi.org/10.1140/epjc/s10052-022-10722-1>.
- [29] M. Atzori Corona, M. Cadeddu, N. Cargioli, F. Dordei, C. Giunti, Y. F. Li, C. A. Ternes, and Y. Y. Zhang, *J. High Energy Phys.* **2022**, 164 (2022), ISSN 1029-8479, URL [https://doi.org/10.1007/JHEP09\(2022\)164](https://doi.org/10.1007/JHEP09(2022)164).
- [30] F. An, G. An, Q. An, V. Antonelli, E. Baussan, J. Beacom, L. Bezrukov, S. Blyth, R. Brugnera, M. B. Avanzini, et al. (JUNO Collaboration), *J. Phys. G: Nucl. Part. Phys.* **43**, 030401 (2016), URL <https://dx.doi.org/10.1088/0954-3899/43/3/030401>.
- [31] A. Popov and A. Studenikin, *Eur. Phys. J. C* **79**, 144 (2019), ISSN 1434-6052, URL <https://doi.org/10.1140/epjc/s10052-019-6657-z>.
- [32] A. Popov and A. Studenikin, *Phys. Rev. D* **103**, 115027 (2021), URL <https://link.aps.org/doi/10.1103/PhysRevD.103.115027>.
- [33] M. Nowakowski, E. A. Paschos, and J. M. Rodríguez, *Eur. J. Phys.* **26**, 545 (2005), URL <https://dx.doi.org/10.1088/0143-0807/26/4/001>.
- [34] S. Navas, C. Amsler, T. Gutsche, C. Hanhart, J. J. Hernández-Rey, C. Lourenço, A. Masoni, M. Mikhasenko, R. E. Mitchell, C. Patrignani, et al. (Particle Data Group Collaboration), *Phys. Rev. D* **110**, 030001 (2024), URL <https://link.aps.org/doi/10.1103/PhysRevD.110.030001>.
- [35] A. I. Ternov, *JETP Letters* **104**, 75 (2016), ISSN 1090-6487, URL <https://doi.org/10.1134/S0021364016140137>.
- [36] A. I. Ternov, *Phys. Rev. D* **94**, 093008 (2016), URL <https://link.aps.org/doi/10.1103/PhysRevD.94.093008>.
- [37] K. S. Babu and R. N. Mohapatra, *Phys. Rev. D* **41**, 271 (1990), URL <https://link.aps.org/doi/10.1103/PhysRevD.41.271>.
- [38] G. G. Raffelt, *Phys. Rep.* **320**, 319 (1999), ISSN 0370-1573, URL <https://www.sciencedirect.com/science/article/pii/S0370157399000745>.
- [39] W. C. Haxton and C. E. Wieman, *Annu. Rev. Nucl. Part. Sci.* **51**, 261 (2001), ISSN 1545-4134, URL <https://www.annualreviews.org/content/journals/10.1146/annurev.nucl.51.101701.132458>.
- [40] C. Giunti and C. W. Kim, *Fundamentals of Neutrino Physics and Astrophysics* (Oxford University Press, 2007), ISBN 9780198508717, URL <https://doi.org/10.1093/acprof:oso/9780198508717.001.0001>.

- [41] W. M. Alberico, S. M. Bilenky, C. Giunti, and K. M. Graczyk, *Phys. Rev. C* **79**, 065204 (2009), URL <https://link.aps.org/doi/10.1103/PhysRevC.79.065204>.
- [42] D. K. Papoulias and T. S. Kosmas, *Adv. High Energy Phys.* **2016**, 1490860 (2016), <https://onlinelibrary.wiley.com/doi/pdf/10.1155/2016/1490860>, URL <https://onlinelibrary.wiley.com/doi/abs/10.1155/2016/1490860>.
- [43] G. T. Garvey, W. C. Louis, and D. H. White, *Phys. Rev. C* **48**, 761 (1993), URL <https://link.aps.org/doi/10.1103/PhysRevC.48.761>.
- [44] J. Liu, R. D. McKeown, and M. J. Ramsey-Musolf, *Phys. Rev. C* **76**, 025202 (2007), URL <https://link.aps.org/doi/10.1103/PhysRevC.76.025202>.
- [45] A. V. Butkevich, *Phys. Rev. D* **107**, 073001 (2023), URL <https://link.aps.org/doi/10.1103/PhysRevD.107.073001>.
- [46] K. A. Kouzakov and A. I. Studenikin, *Phys. Rev. D* **95**, 055013 (2017), URL <https://link.aps.org/doi/10.1103/PhysRevD.95.055013>.
- [47] M. A. Corona, W. M. Bonivento, M. Cadeddu, N. Cargioli, and F. Dordei, *Phys. Rev. D* **107**, 053001 (2023), URL <https://link.aps.org/doi/10.1103/PhysRevD.107.053001>.
- [48] E. Aprile, J. Aalbers, F. Agostini, M. Alfonsi, L. Althueser, F. D. Amaro, V. C. Antochi, E. Angelino, J. R. Angevaere, F. Arneodo, et al. (XENON Collaboration), *Phys. Rev. D* **102**, 072004 (2020), URL <https://link.aps.org/doi/10.1103/PhysRevD.102.072004>.